

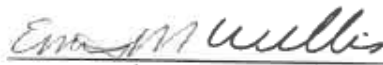
**Simulation of Charge Collection to Spacecraft
Surfaces: Freja Satellite**

Olivia Hope Wolfley

Marshall Space Flight Center

May 4, 2018

**Reviewed by NASA Mentor
Emily Moon Willis
EV44 – Natural Environments Branch**



Mentor Signature Here

Simulation of Charge Collection to Spacecraft Surfaces: Freja Satellite

Olivia H. Wolfley¹

Rose State College, Midwest City, OK, 73110

As spacecraft travel through space plasma, spacecraft surfaces become charged by the collection of charged particles. This process is referred to as Surface Charging. These charges can be detrimental to the vehicle's electronic subsystems as they present a threat of electrostatic discharge (ESD) to onboard circuitry. The process of Surface Charging is complex and is affected by many elements. The charging of each surface is unique. The potential of an individual surface is dependent upon many variables including but not limited to the surface's geometry, material and its location. Each surface also has unique interactions with the surrounding plasma. Other factors that play large roles in the charging process is the density and temperature of plasma ions and electrons. Using Nascap-2k, a model of the Freja satellite has been constructed, and its auroral plasma environment has been imitated to simulate surface charging characteristics. The charging process of the Freja satellite has been modeled iteratively with incremental changes in both the Maxwellian electron temperature (eV) as well as the Gaussian electron energy (eV). This study provides an analysis of the sensitivity between spacecraft surface charging and these two primary variables of electron differential flux.

Nomenclature

σ	=	Secondary Electron Coefficient
<i>ESD</i>	=	Electrostatic Discharge
LEO	=	Low Earth Orbit
<i>SEE</i>	=	Secondary Electron Emission Yield
EP_{max}	=	Secondary Electron Emission Energy
eV	=	Electron Volts
I	=	Current
I_i	=	Incident Ion Current
I_e	=	Incident Electron Current
I_{be}	=	Backscattered Electron Current
I_{se}	=	Secondary Electron Current
I_{si}	=	Secondary Ion Current
I_{ph}	=	Photoelectron Emission Current
I_T	=	Total Current

I. Introduction

Nascap-2k is a Graphical User Interface that computes and portrays charging characteristics for satellites in specific environments. Nascap-2k was utilized in this sensitivity study of the Freja spacecraft's charging characteristics. The program's software takes the unique variables of surfaces, ions, electrons, and many other elements into account when calculating results. The Freja spacecraft's charging process was first simulated in a severe-case environment. After the severe-case simulation data was recorded, the environment was manipulated to then analyze the influential factors of the craft's charging. The variables of the electron differential flux ($m^{-2}s^{-1}eV^{-1}$) were incrementally decreased and compared against the actuated change in differential potential (V). Throughout this

¹ NASA Intern, EV-44 Natural Environments Branch, Marshal Space Flight Center, Rose State College.

study, differential potential is defined as the difference between the potential of the surface material and the potential of the chassis. This study concentrates on two main variables, these are Maxwellian electron temperature (eV), and Gaussian electron energy (eV). This paper provides an analysis of the relationship between these two variables and the differential potential (V) of the Freja spacecraft.

II. The Freja Satellite

A. Background

The Freja satellite is of Swedish origin and was launched into space on October 6, 1992¹. It now orbits earth with an inclination of $\sim 63^\circ$ and an altitude varying from 601km over the southern hemisphere to 1756km over the northern hemisphere where its polar orbit passes through the northern auroral region¹.

Freja satellite specifications were gathered from a report of the Swedish Institute of Space Physics². The satellite has a diameter of approximately two meters and a height of just under a half meter. The craft consists of two tiers connected by an aluminum duct and four support walls all propagated from the central duct. The uppermost tier measures 2.2 meters in diameter and holds eight identic solar panels while the lower tier measures only 1.2 meters and acts as the base for the instrument bay and anchors an array of scientific equipment.

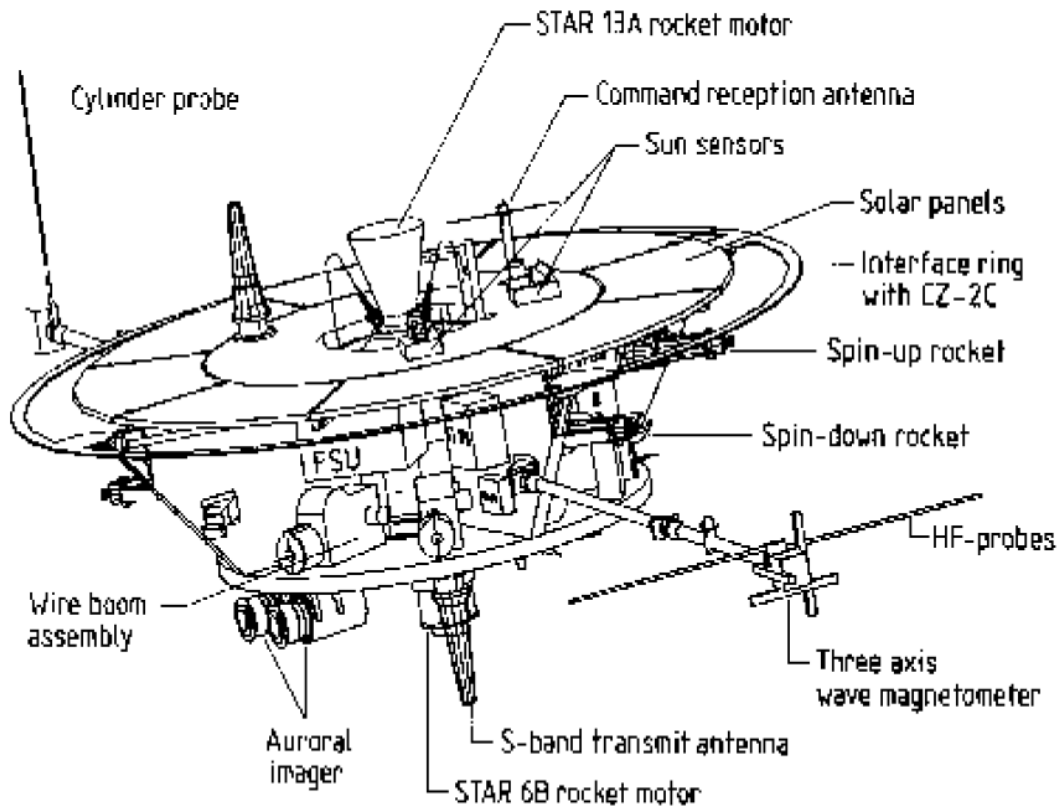


Figure 1. Schematic of the Freja satellite and its instruments.²

B. Modelling the Spacecraft

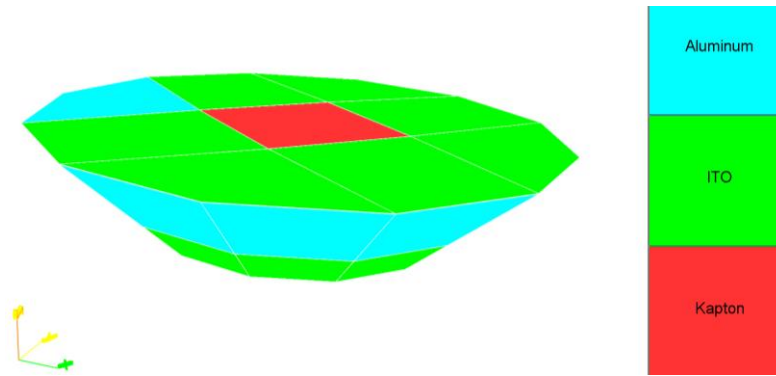


Figure 2. Simplified Model of Freja Spacecraft

Figure 2 shows the primitive replica created through Nascap’s Object Toolkit. The true satellite is made up of many materials some of which have only minor distinctions between each other. However, for the purposes of this sensitivity study only three materials are included in the simplified model of our satellite: Kapton, Aluminum and Indium tin oxide (ITO). As Kapton is a dielectric material, it has been specified to have a dielectric constant of 3.5. Both Aluminum and ITO are conductors and have been specified to have a dielectric constant of 1. One of the most influential factors of surface charging is the Secondary Electron Emission yield (SEE) of each material. A secondary electron is one that is emitted from a surface due to the collision of an incident electron with the same surface. The SEE coefficient σ is defined as the ratio of ejected electrons per incident electron³. The SEE energy EP_{max} is the energy of the incident electrons at which the SEE coefficient is highest. While the SEE energies and coefficients for both Kapton and Aluminum have been provided by Nascap, these values for ITO were gathered from a paper of Case

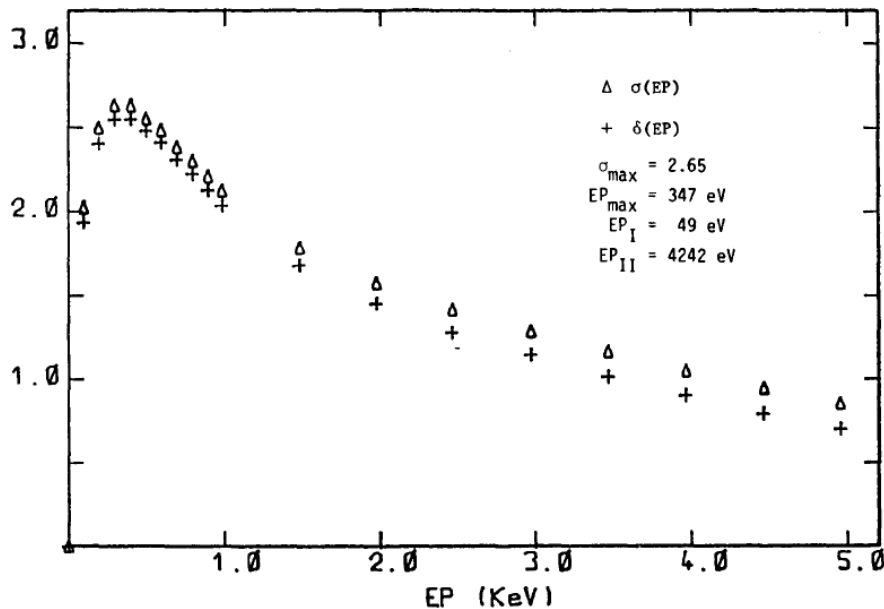


Figure 3. SEE coefficients for ITO.³

Western Reserve University.³ As shown in figure 3, the SEE coefficient for ITO is 2.65 when the incident electron energy is 0.347 keV.

The charging process of the modelled Freja satellite was found to have a high sensitivity to the SEE parameters of the ITO material. For example, independently changing the SEE energy from 0.347 keV to 0.4 keV caused the surface potential of the Kapton to positively increase from -928.7 volts to -792.9 volts. As the model consists primarily of ITO, this substantial reactance to the SEE parameters of ITO may be due to the abundance of the material.

III. Charging Process

Atmospheric plasma is a gas consisting of charged electrons and ions that are traveling in an omnidirectional manner⁴. The ions throughout Freja’s LEO/auroral environment are predominantly ionized oxygen (O^+), whereas the most frequent ion in the plasma above LEO is ionized hydrogen (H^+).⁴

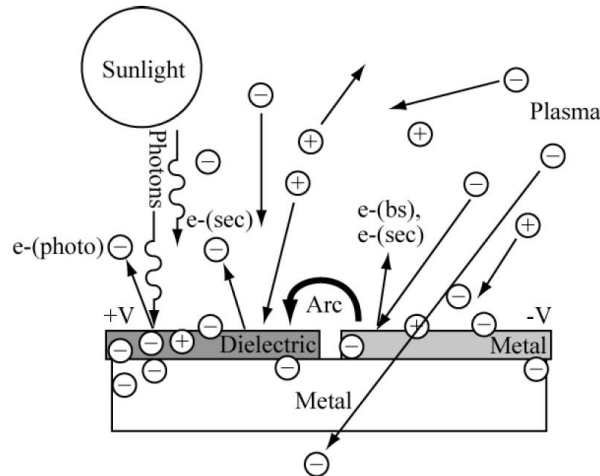


Figure 4. Illustration of plasma interactions.⁴

As satellites travel through this ionized plasma, these charged particles begin to collect on the satellite’s surfaces creating electric currents. Electric current is also created when the incoming of electrons and ions cause the outgoing of ions and electrons away from the surface. These ejected particles are known as secondary ions, secondary electrons and backscattered electrons. Another process that causes an additional current is the incoming of photons from sunlight that causes electrons to be emitted from the contact surface. This is known as photoemission. Table 1 conveys the charge associated with each of these particle induced electric currents.

Positive Current (+)	Negative Current (-)
Incident Ions	Incident Electrons
Secondary Electrons	Secondary Ions
Backscattered Electrons	
Photoelectron Emissions	

Table 1. Potentials of current contribution created from charged particle interactions.

It is the summation of these collective currents that provides the total current of each surface⁵.

$$I_T = I_i + I_{se} + I_{be} + I_{ph} - I_e - I_{si} \quad (1)$$

When the summation equals zero, there is equilibrium among the currents and no further charging is occurring⁵. It is the balance of these electric currents that is the cornerstone of the surface charging process⁵.

$$\sum I_k = I_T = 0 \tag{2}$$

IV. Environment Parameters

As surface currents are created from incident particles, the flux of these particles is a prominent proponent in the charging process. This study focuses on the variables of the electron differential flux ($m^{-2}s^{-1}eV^{-1}$) given by equation 3. The variables of this equation make up the parameters of Nascap’s adjustable auroral environment tab as shown in figure 4. These parameters have been broken into four contributing components, Low Energy, Maxwellian, Gaussian, and Power Law. It is by modifying these parameters that a simulated environment has been created in which to model Freja’s charging events. The variables at the focus of this study have been Maxwellian temperature (θ_{max}) and Gaussian energy (E_{gauss}).

$$Flux(E) = \sqrt{\frac{e}{2\pi\theta m_e}} n \exp\left(-\frac{E}{\theta}\right) + \pi\delta_{max} E \exp\left(-\frac{E}{\theta_{max}}\right) + \pi\delta_{gauss} E \exp\left(-\left(\frac{E_{gauss}-E}{\Delta}\right)^2\right) + \pi\delta_{power} E^{-\alpha} \tag{3}$$

where δ_{max} is the coefficient of the Maxwellian component, δ_{gauss} and δ_{power} are the coefficients of the Gaussian and Power Law components respectively, e is the charge of the electron, m_e is the mass of the electron, α is the is the exponent of the Power Law component, Δ is the width of the Gaussian component and n is the density of the Low Energy component.⁶ Also, while θ is the temperature of the low energy plasma, θ_{max} is the temperature of the high energy plasma and is a more influential variable of the flux as the ambient plasma in an auroral environment has high energy particles.⁶

Auroral Environment

Auroral Environment Plasma: User Defined

Low Energy
 Density (m⁻³): 4.710E5
 Temperature (eV): 0.300
 Debye Length (m): 5.933
 E. Current (Am⁻²): 6.915E-9
 Ion Current (Am⁻²): 5.143E-11

Maxwellian
 E. Current(Am⁻²): 2.312E-6
 Temperature (eV): 8000.
 Density (m⁻³): 9.592E5
 Coefficient: 7.177E4

Gaussian
 E. Current(Am⁻²): 1.913E-7
 Energy (eV): 1.100E4
 Width (eV): 1500.
 Density (m⁻³): 8.240E4
 Coefficient: 1.300E4

Power Law
 E. Current(Am⁻²): 3.634E-7
 1st Energy (eV): 1000.
 2nd Energy (eV): 2.000E4
 Exponent: 2.000
 Density (m⁻³): 3.361E5
 Coefficient: 7.600E14

Sun
 Direction to Sun: X:0.0, Y:0.0, Z:0.0
 Relative* Sun Intensity: 0.0
 *(value at Spacecraft) / (value at Earth Orbit)

Magnetic Field (T)
 Bx:0.0, By:0.0, Bz:0.0

Spacecraft Velocity with Respect to Plasma (m/s)
 Vx:0.0, Vy:0.0, Vz:7500.

Type	Mass (amu)	Charge (C)	%
Electron	5.486E-4	-1.602E-19	100.0
Oxygen	16.00	1.602E-19	91.00
HYDROGEN	1.000	1.602E-19	9.000

Add Species, Delete Species

Figure 5. Nascap Auroral Environment Parameters Tab

V. Process of Data Collection

Through Nascap, the parameters of the differential flux were first formulated to resemble a severe-case environment. The initial values are shown in figure 5. This base environment produced surface potentials on the order of -1000 volts with respect to the surrounding plasma ground and differential potentials on the order of -500 volts with respect to the chassis. Repetitive simulations were run while incrementing independent variables. For each iteration the greatest resulting differential potential values were recorded. The data is presented through graphs where the spacecraft's differential potential values are plotted against the corresponding independent variable.

Figure 6 displays the results from a simulation series where the Maxwellian Temperature was decreased by 500 electron volts with each iteration. Figure 7 displays the results from another repetition of simulations where the Gaussian energy was decreased by 10,000 electron volts with each iteration. Series of simulations were conducted where both small and large variable increments were used. The data graphs of these additional simulation sets can be found in Appendices A and B.

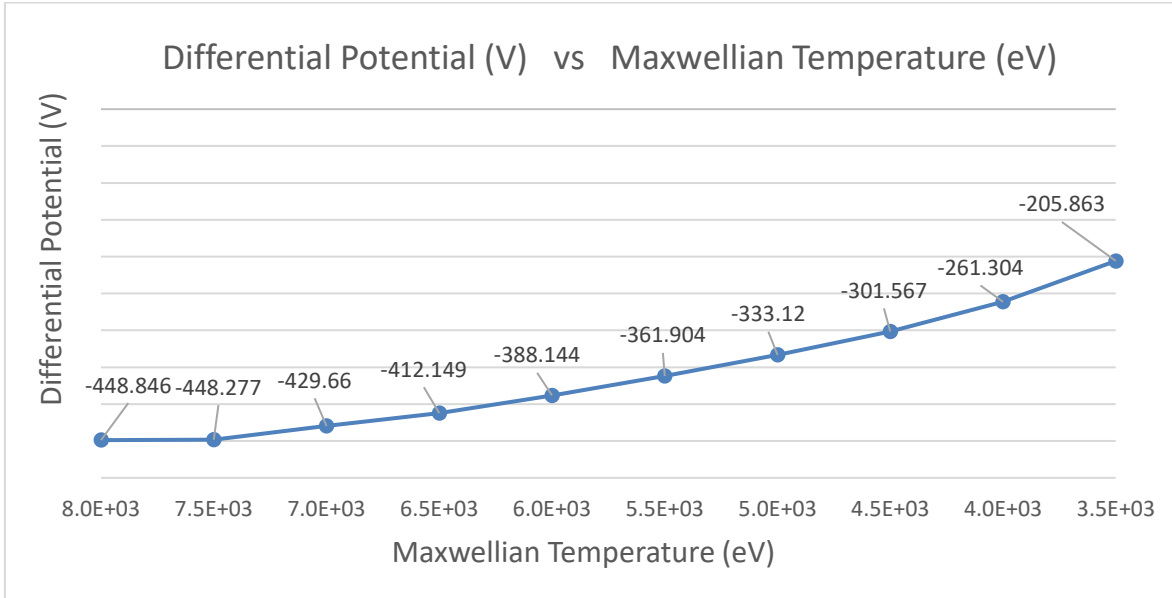


Figure 6. Differential potential values plotted against the corresponding Maxwellian Temperature values. Maxwellian temperature ranging from 8.0×10^3 (eV) to 3.5×10^3 (eV).

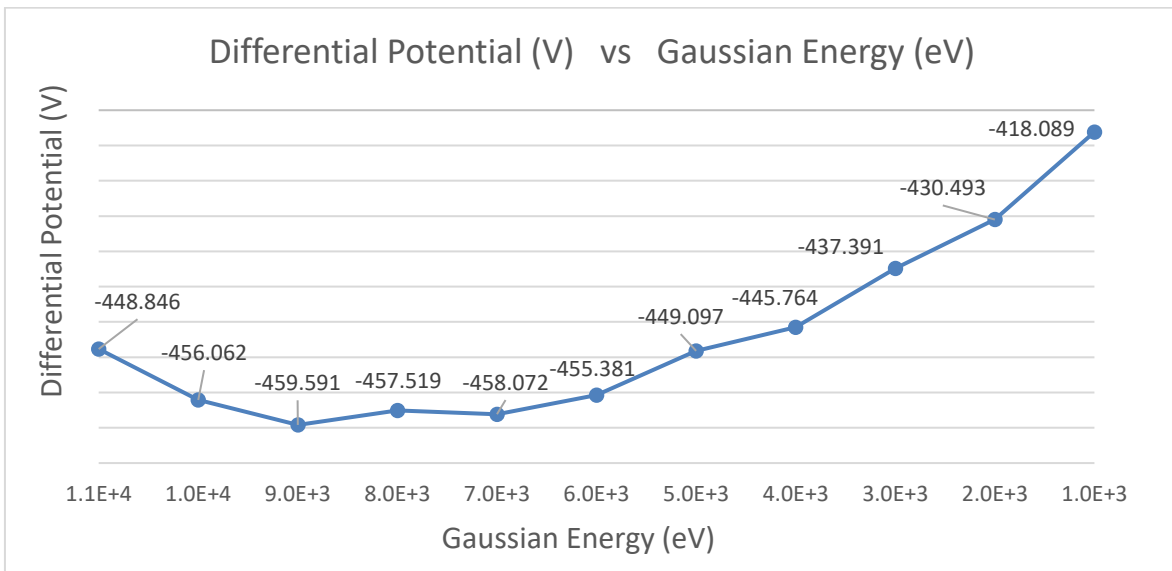


Figure 7. Differential potential values plotted against the corresponding Gaussian energy values. Gaussian energy ranging from 1.1×10^4 (eV) to 1.0×10^3 (eV).

VI. Discussion

Changes in Maxwellian temperature correspond with differential potential values in a somewhat linear fashion. As the temperature was decreased, the differential potential also decreased in terms of magnitude, however in terms of charge the differential potential increased as it approached positivity. Gaussian energy appears to have a non-linear relationship with differential potentials. The values that were produced from the simulations where the

Gaussian energy was manipulated were slightly more erratic than those produced from manipulating Maxwellian temperature. As shown in Figure 7, the differential potential values first decrease in concert with the Gaussian energy then, as the energy reaches ~8000 (eV), the differential potentials begin to increase. As shown in Figure 9, the increment size of the Gaussian energy was reduced and unpredictable differential potential values continued to be generated. Gaussian energy’s influence on differential potential is not yet fully understood. While both Gaussian energy and Maxwellian temperature prove to be significant factors in the surface charging process, more research needs to be conducted to better understand the relationship between these variables of electron differential flux and the differential potentials of spacecraft surfaces.

Appendix

A. Maxwellian Simulation Data

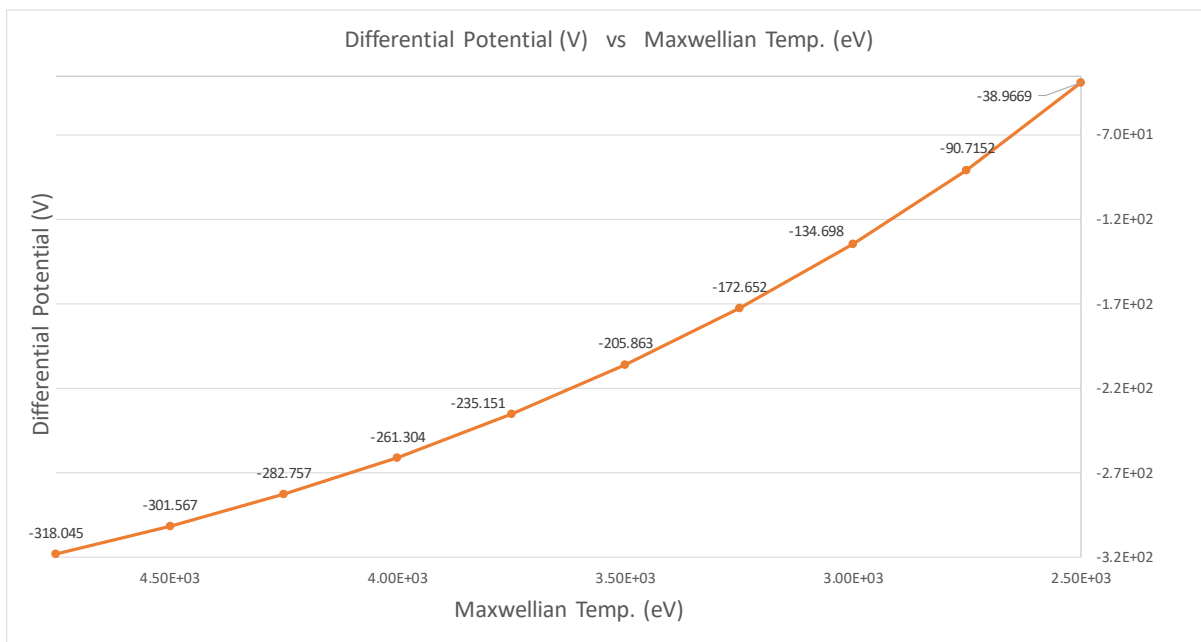


Figure 8. Maxwellian temperature ranging from 4.5×10^3 (eV) to 2.5×10^3 (eV).

B. Gaussian Simulation Data

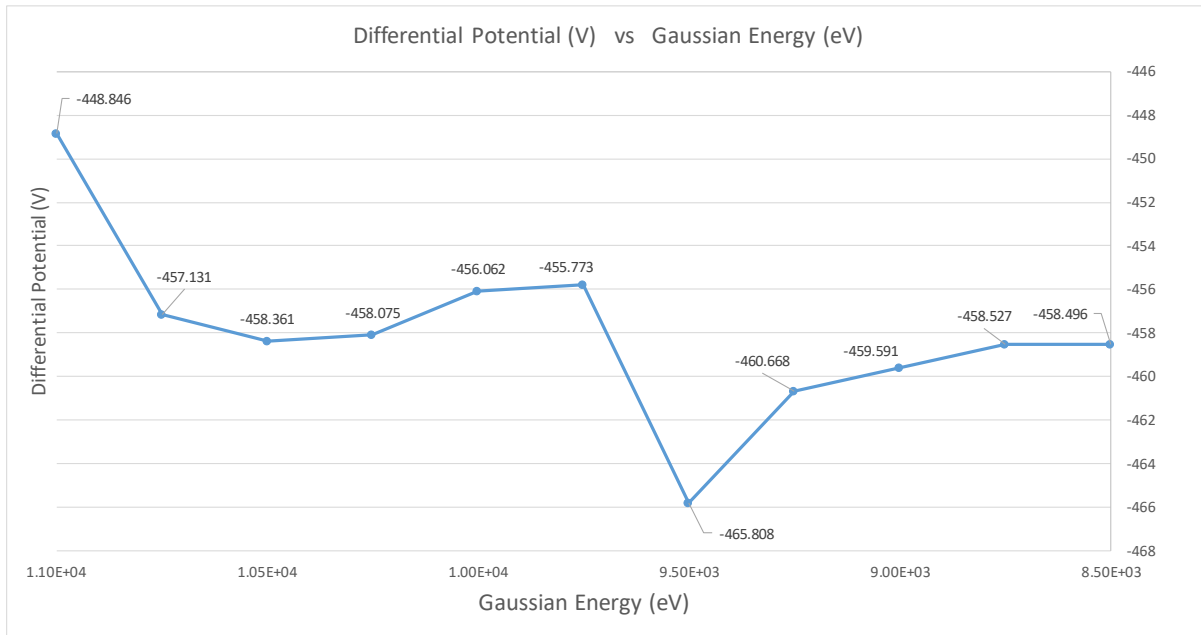


Figure 9. Gaussian energy ranging from 1.1×10^4 (eV) to 8.5×10^3 (eV).

Acknowledgments

Many thanks to Emily M. Willis for her mentorship and willingness to entertain the wonderings of a young engineer. I would also like to thank the EV44 Natural Environments Branch and Adison Nordstrom for her assistance throughout this project. Also, thanks to University Space Research Association for their funding of this internship.

References

¹Andersson, L., Carrozi, T., Eriksson, I. A., Holback, B., Laakso, H., Wahlund, J-E., and Wedin, L. J., “Analysis of Freja Charging Events: Statistical Occurrence of Charging Events,” SPEE-WP130-TN, Feb. 1999.

²Andre, M., “The Freja Scientific Satellite,” Swedish Institute of Space Physics, IRF Scientific Report 214, Kiruna 1993.

³Gordon, W. L., Hoffman, R.W., Krainsky, I., and Lundin, W., “Secondary Electron Emission Yields,” NASA NSG-3197.

⁴Garrett, H.B., and Whittlesey, A.C., “Guide to Mitigating Spacecraft Charging Effects,” Jet Propulsion Laboratory and California Institute of Technology, June 2011.

⁵Eriksson, I. A., Holback, B., Laakso, H., Wahlund, J-E., and Wedin, L., “Analysis of Freja Charging Events: Modelling of Freja Observations by Spacecraft Charging Codes,” SPEE-WP120-TN, Dec. 1998.

⁶Davis, V.A., Gardner, B.M., Mandell, M.J., “Nascap-2k Version 4.3 User’s Manual,” AFRL-RV-PS-TR-2017-XXXX, Dec. 2016.

